R. TARANKO, E. TARANKO, M. PIŁAT

Charge Fluctuation in Random Binary Alloys: Influence of a Short–Range–Order within Cluster–Bethe–Lattice Approach.

Fluktuacje ładunkowe w stopach dwuskładnikowych: wpływ uporządkowania bliskiego zasięgu w ramach formalizmu „cluster–Bethe–lattice"

Зарядовые флуктуации в бинарных сплавах: влияние упорядочения ближнего порядка в рамках формализма решётки типа „кластер-Бете"

1. INTRODUCTION

Usually, in the works on the electronic structure of the disordered alloys one concentrates on calculating the configuration average of the local density of states. Nevertheless, sites in a random alloys are not equivalent due to random fluctuations in the local atomic environment. Additionally, alloys generally have atomic short–range–order and for that reason the average value of the site's occupation number can be different from the occupation number of any particular site. It seems, that the static fluctuations of electronic charge density in metallic binary alloys has been overlooked in literature on alloys properties and only in work by Ling and Gelatt [1] these problems were studied intensively. On the other hand, the similar problems (from mathematical point of view) i.e. the magnetic moments fluctuations and its concentration dependence in ferromagnetic alloys were studied in detail by Hamada and Miwa [2]. Also many experiments have studied the effect of the local atomic environment on the local magnetic moments (see References in Ref. [2]). Among the experimental probes available to check or investigate charge fluctuations in

metallic alloys are, for example, core–level energy shift using X–ray photoemission spectroscopy, Mössbauer isomer–shift measurements, the optical measurements of the defect states in the semiconductors and others.

In a work by Ling and Gelatt [1] the static charge fluctuations were investigated by means of three different calculational techniques. These techniques were a weak–scattering perturbation expansion, a dilute–alloy perturbation expansion and a coherent potential approximation — perturbation theory. We can see, that the results obtained from these calculations are valid only in a narrow range of some parameters and do not take into account the short–range–order. It should be noted that actual alloys generally have atomic short–range–order. For that reason it would be interesting and at the same time very important to investigate the influence of the atomic short–range–order on the static charge fluctuations in the binary metallic alloys. More exact calculations of the charge fluctuations can be also very useful in estimation of the broadening of a core–level linewidth observed in X–ray photoemission (see also for experimental evidence of a fluctuating charge state in cupric oxide extracted from the X–ray photoelectron spectroscopic study [3]).

The paper is organized as follows. In the next section we give the general expression for static charge fluctuations. In Sec. III we present the method needed for calculation of the alloy electronic characteristics with the short–range–order included. The concrete evaluations of the different alloy's electronic characteristics and charge fluctuations are performed in Sec. IV.

2. THEORY

2.1. Charge fluctuations

In this section we present several basic relations concerning the charge fluctuations in alloys [1]. For each microscopic arrangement of a type–A and type–B atoms (here we consider the substitutional binary alloys), all information about the electronic structure is contained in the Green's function

$$G(E) = (E - H)^{-1} \tag{1}$$

where H is a model alloy's Hamiltonian. This Green's function depends on a specific arrangement of a constituent atoms. Having in hand G one can calculate the site–projected density of states according to the formula

$$N_i(E) = -\frac{1}{\pi} \text{ Im Tr } (|i><i| G(E^+)) \tag{2}$$

where $|i>$ is the Wannier state at i–th site and $E^+ = E + i\varepsilon$, $\varepsilon > 0$. In order to calculate the site occupation number one have to integrate over energy the site–projected density of states

$$n_i = \int_{-\infty}^{+\infty} n_F(E) N_i(E) \, dE \tag{3}$$

where $n_F(E)$ is the Fermi distribution function. Usually, as a main quantity characterizing the charge distribution in an alloy, the average value of the site occupation number is calculated

$$n_i^{A(B)} = \int_{-\infty}^{E_F} < N_i(E) >_{i=A(B)} dE \qquad (4)$$

where $< \ldots >_{i=A}$ denotes a restricted configuration average, i.e. a configuration-averaging process is performed only over those arrangement with A atom at the origin. Here we confined ourselves to the case of zero absolute temperature, so the chemical potential is replaced by the Fermi energy E_F. Of course, $n_i^{A(B)}$ represents the charge distribution rather in a crude manner. For that reason we have to calculate another quantity which can better reflect the true charge distribution. In this paper we are going to investigate the mean–square fluctuations in the site occupation numbers and according to the formulas given in [1] we can write

$$\Delta n_A^2 \equiv \langle (n_i - < n_i >_{i=A})^2 \rangle_{i=A} =$$

$$= \int_{-\infty}^{E_F} dE \int_{-\infty}^{E_F} dE' \langle (N_i(E) - < N_i(E) >_{i=A}) (N_i(E') - < N_i(E') >_{i=A}) \rangle_{i=A}$$

$$(5)$$

or

$$\Delta n_A^2 = \frac{1}{\pi^2} \int_{-\infty}^{E_F} dE \int_{-\infty}^{E_F} dE' < (\operatorname{Im} \operatorname{Tr} |i><i|G(E) - \operatorname{Im} \operatorname{Tr} |i><i|G^{i=A}(E))$$

$$(\operatorname{Im} \operatorname{Tr} |i><i|G(E') - \operatorname{Im} \operatorname{Tr} |i><i|G^{i=A}(E')) >_{i=A} \qquad (6)$$

where $G^{i=A}(E)$ denotes the alloy Green's function in a case for which the i–th site is occupied by A–atom.

2.2. Cluster–Bethe–lattice method

In order to calculate the influence of the short–range–order on the mean–square charge fluctuations (MSCF) according to the formula (6) we have to calculate a restricted average values of the product of two Green's function.

In a study of disordered systems a widely accepted concept is that of an effective medium. More specifically, a homogeneous medium is chosen in such a way that the average behaviour of an ensemble of disordered samples is reproduced in the behaviour of one homogeneous sample. A widely used example of such approach is the coherent potential approximation (CPA) [4], or its generalizations, for example, the homomorphic CPA [5], the self–consistent self–energy approximation [6], the molecular CPA [7], the travelling cluster approximation (see [8] and references therein), and others. Here we use the cluster–Bethe–lattice method (CBL) connected with a single site CPA, which allows us to calculate in a relatively simple way the alloy Green's function with short–range–order included. The Bethe–lattice approximation used, for example, for the calculation of the partition function of a

magnetic systems [9] and for which an exact analytic treatment is possible for simple tight–binding Hamiltonians. It consists in substituting for the infinite periodic lattice an infinite system of connected atoms with the same coordination number as the lattice of interest, but without closed rings of bounds. This lattice has the property that the one–particle Green's function at a given site can be expressed in terms of the Green's function at the preceding site in the lattice. The Bethe–lattice approximation is exact in one–dimensional systems and is good in low coordination three–dimensional lattices. For a closed–packed structures one have use a better approximation, usually the Husimi cactus model which consists of an infinite system of connected tetrahedra [10, 11]. In the CBL approximation a small cluster of atoms is treated exactly and the remainder of the alloy is simulated by attaching Bethe–lattice of the same coordination number to the "dangling bounds" of the atoms at the surface of the cluster. The alloy Bethe–lattice can be, in a next step, replaced by the effective Bethe–lattice with the effective fields calculated within the single site approximation.

As was already mentioned, we shall use the CBL method for calculation of the Green's function conditional average values appearing in Eq. (6). Let us consider a cluster of nine atoms (a smallest cluster of atoms for bcc lattice) which is described by the single–particle tight–binding (single–band) Hamiltonian with a hopping integrals V_{ij} taking values V_{AA}, V_{BB}, V_{AB}, and V_{BA} depending on whether the i–th and j–th atoms are both of class A, both of class B or one of each class, respectively. The short–range–order is introduced through the independent order parameter P_{AB} (additional to the concentration of the one of a constituent atoms). This parameter denotes the possibility of finding a type–B atom as a nearest neighbour to a type–A atom. Six parameters, x, $y = 1 - x$, P_{AA}, P_{AB}, P_{BA} and P_{BB} describing the concentration of the type–A and type–B atoms and the degree of correlation in the occupation of a neighbouring sites can be expressed (because of symmetry and normalization conditions) by two independent parameters. It is most convenient to choose these to be x and p, where p is introduced by the following relations (see, for comparison, [2, 12 – 17])

$$P_{AA} = x + (1 - x)p$$

$$P_{AB} = (1 - x)(1 - p)$$

$$P_{BA} = x(1 - p)$$

$$P_{BB} = 1 - x(1 - p).$$

(7)

Note, that completely random disorder occurs when the short–range–order parameter p is equal zero. For $p = -1$, $x = 0.5$ perfect long–range–order occurs and for $p = 1$ the alloy separates into pure–A and pure–B phases (segregation limit). It should be noted that the local order is extended only over a small region depending upon both x and p and usually extends to the fifth nearest–neighbours [18].

In the Hamiltonian describing the Bethe–lattice alloy we have taken the average hopping matrix element in the form [14]

$$\overline{V} = x(P_{AA} \cdot V_{AA} + P_{AB} \cdot V_{AB}) + (1 - x)(P_{BB} \cdot V_{BB} + P_{BA} \cdot V_{BA}) \qquad (8)$$

and the diagonal self–energy $\sigma(E)$ was introduced to replace the random diagonal elements by site independent value [4]. Following the transfer matrix method (see, for comparison, [19]) and coherent potential approximation [4] the self–energy can be calculated from following equations:

$$x(\varepsilon_A - \sigma(E))(1 - (\varepsilon_A - \sigma(E))\overline{G_{00}})^{-1} +$$

$$(1 - x)(\varepsilon_B - \sigma(E))(1 - (\varepsilon_B - \sigma(E))\overline{G_{00}})^{-1} = 0 \qquad (9)$$

$$\overline{G_{00}} = x\overline{G_{00}^A} + (1 - x)\overline{G_{00}^B} \qquad (10)$$

$$\overline{G_{00}^A} = (E - \varepsilon_A - Z\overline{V}T)^{-1} \qquad (11)$$

$$\overline{G_{00}^B} = (E - \varepsilon_B - Z\overline{V}T)^{-1} \qquad (11)$$

where the transfer matrix T reads as

$$T = \frac{E - \sigma(E) \pm \sqrt{(E - \sigma(E))^2 - 32\overline{V}^2}}{14\overline{V}} \qquad (13)$$

Here, $\overline{G_{00}}$ is a diagonal matrix element of the average Green's function at site „0"

and $\overline{G_{00}^A}$ is a diagonal matrix element of the average Green's function at site „0"

when this site is occupied by type–A atom.

In the next step we consider a cluster of atoms (in our case $Z + 1$ atoms, $Z = 8$) and to each of the surface atom in this cluster a Bethe–lattice is connected. From the Dyson equation for a Green's function we have [14]

$$(E - \varepsilon_0)G_{00} = 1 + \sum_{i=1}^{Z} V_{0i}G_{i0} \qquad (14)$$

$$(E - \varepsilon_i)G_{i0} = V_{i0}G_{00} + (Z - 1)\overline{V}_i K_i^{(1)}, \quad i = 1, \ldots, Z \qquad (15)$$

$$(E - \sigma(E))K_i^{(1)} = \overline{V}_i G_{i0} + (Z - 1)\overline{V} K_i^{(2)}, \quad i = 1, \ldots, Z \qquad (16)$$

$$(E - \sigma(E))K_i^{(2)} = \overline{V} K_i^{(1)} + (Z - 1)\overline{V} K_i^{(3)}, \quad i = 1, \ldots, Z \qquad (17)$$

$$\vdots$$

where $K_i^{(j)}$ is a Green's function connecting the i-th atom in the j-th level of the Bethe lattice with the central atom, $\overline{V}_i = \overline{V}_A$ or $\overline{V}_B$ depending on a type of atom occupying the i-th lattice site and

$$\begin{aligned} \overline{V}_A &= P_{AA}V_{AA} + P_{AB}V_{AB} \\ \overline{V}_B &= P_{BB}V_{BB} + P_{BA}V_{BA} \end{aligned} \qquad (18)$$

Having in hand equations (7 – 18) and the expression for the average value of a Green's function

$$\langle G_{00}(E) \rangle_{0=A(B)} = \sum_{i=0}^{Z} \binom{8}{n_A} P_{AA}^{n_{A(B)}} P_{AB}^{Z-n_{A(B)}} G_{00}^{A(n_A, Z-n_A)}(E) \quad (19)$$

we are able to calculate the average values needed for calculation of the charge fluctuations. Eq. (6). Here, $G_{00}^{A(n_A, Z-n_A)}(E)$ denotes the diagonal matrix element of a Greens function G, Eq. (1), in a case when in the central site of a cluster is located a type–A atom surrounded by n_A type–A atoms and $(Z - n_A)$ type–B atoms (first neighbours). Additionally, with each of these boundary atoms the effective Bethe–lattice is connected. The explicit expression for $G_{00}^{A(n_A, Z-n_A)}(E)$ is as follows (cf. [14, 15]):

$$G_{00}^{A(n_A, Z-n_A)}(E) = \left[(E - \varepsilon_A) - \frac{n_A V_{AA}^2}{X} - \frac{(8 - n_A)V_{AB}^2}{X} \right]^{-1} \quad (20)$$

$$X = (E - \varepsilon_A) - \frac{7\overline{V}_A^2}{E - \sigma(E) - \dfrac{7\overline{V}}{s}} , \quad (21)$$

$$Y = (E - \varepsilon_B) - \frac{7\overline{V}_B^2}{E - \sigma(E) - \dfrac{7\overline{V}}{s}} , \quad (22)$$

$$s = \frac{E - \sigma(E) \pm \sqrt{(E - \sigma(E))^2 - 28\overline{V}^2}}{2\overline{V}} . \quad (23)$$

To the end, the expression for the mean–square fluctuations in the site occupation numbers reads as [1]:.

$$\Delta n_{A(B)}^2 = \frac{1}{\pi^2} \left(\int_{-\infty}^{E_F} dE \int_{-\infty}^{E_F} dE' < \text{Im } G_{00}(E) \cdot \text{Im } G_{00}(E') >_{0=A(B)} - \right.$$

$$\left. - (\int_{-\infty}^{E_F} dE < \text{Im } G_{00}(E) >_{0=A(B)})^2 \right) , \quad (24)$$

where the calculations of the conditional averages are performed according to the formula (19).

3. NUMERICAL RESULTS AND DISCUSSION

In this section we apply the method of Sec. 2 to study the charge fluctuation in an alloy with the diagonal, off–diagonal disorder and short–range–order included. We present also the density of states corresponding to a single type–A and type–B

atoms located inside of a nine atoms cluster and surrounded by the effective Bethe–lattice. In order to better visualize the set of a short–range–order parameters p and a type–A atoms concentrations x, for which the calculations have been performed, we present its as a small circles in Fig. 1 in the region of (x, p) parameters (see for comparation, [12]). As one can see, we choose such values of the short–range–order
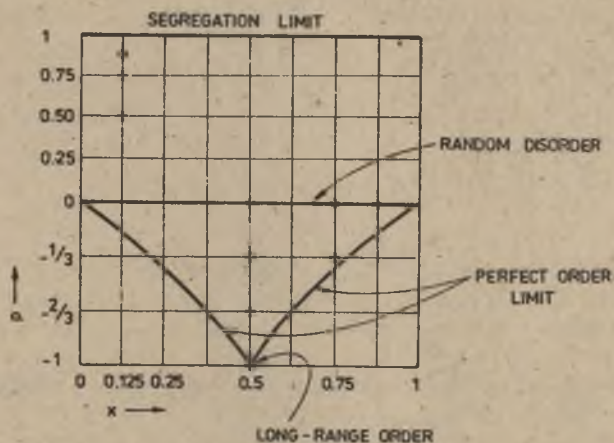

Fig. 1. Allowed range of the short–range–order parameter p vs. concentration of the type–A atoms x. The small circles denote points for which calculations of the charge fluctuations were done

parameters in order to investigate interesting for our study phenomena at various limiting cases, i.e. near the segregation limit (for constant value of x), at random disorder (for increasing values of x), for constant value of x and increasing values of p and in additional positions near the perfect order limit. In our calculations we have taken $\varepsilon_A = -\varepsilon_B = 2.0$, 1.0 or 0.5 eV and for V_{AA}, $V_{AB} = V_{BA}$ and for V_{BB} we have chosen the set of values $(1.0, 1.1, 1.2)$ eV (see, for comparison [13, 18]). In all cases presented here we have only one energy band (without localized states outside of the band limits).

In Figs. (2–6) we have drawn the local density of states (LDOS) corresponding to the central type–A and type–B atoms of the nine–atoms cluster–Bethe–lattice system for all possible distributions of the atoms in a cluster. Additionally, we have presented also the average LDOS – the broken line. From Figs. (2, 3) one can observe the changes of LDOS for equal concentrations of the constituent atoms and for disorder parameter going from the value corresponding to the long–range–order to random disorder case. Note that in Fig. 2. one has $P_{AA} = P_{BB} = 0$, $P_{AB} = P_{BA} = 1$ and in Fig. 3, $P_{AA} = P_{AB} = P_{BA} = P_{BB} = 0.5$. In Fig. 2, for type–$B$ atom in a centrum of the cluster constructed from type–B atoms only, we find a pronounced peak in lower part of the energy band. The strength of this peak
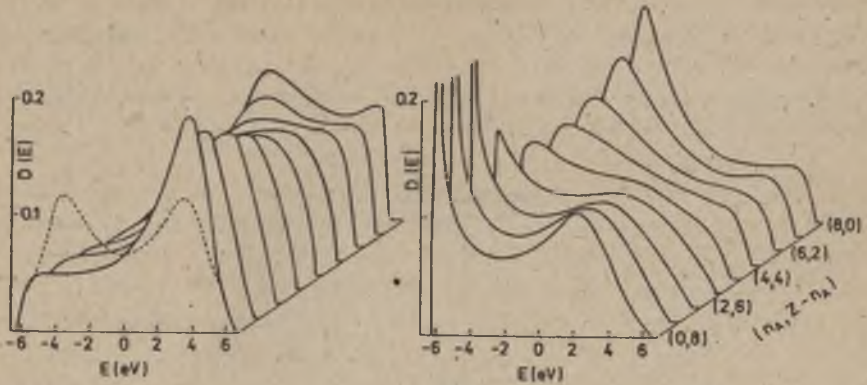
Fig. 2. Local density of states corresponding to the central type–A atom (left–hand side) and type–B atom (right–hand side) in the nine–atoms cluster surrounded by effective Bethe–lattice. The number of different atoms in the cluster is indicated as (n_A, n_B) for $n_A = 0, 1, \ldots, 8$, where $n_B = Z - n_A$, $Z = 8$. The broken curve denotes the average local density of states. The concentration of type–A atoms $x = 0.5$ and short–range–order parameter $p = -1$

gradually decreases as we move from long–range–order limit towards the random disorder. Also, the average LDOS changes significantly. For a long–range–order we have symmetrical LDOS which changes into rather structureless curve for random disordered alloys. Looking on Figs. (3 – 5), one can observe a continuous changes of LDOS with increasing value of a type–A atom concentration.

Here we have $P_{AA} = P_{AB} = P_{BA} = P_{BB} = 0.5$, $x = 0.5$ for Fig. (3), $P_{AA} = P_{BA} = 0.75$, $P_{BB} = P_{AB} = 0.25$, $x = 0.75$ for Fig. (4) and $P_{AA} = P_{BA} = 0.825$, $P_{AB} = P_{BB} = 0.125$, $x = 0.875$ for Fig. (5). There is a noticeable change (with increasing value of x) of the LDOS curves corresponding to all types of the clusters. The average LDOS has a two–peaked structure in the vicinity of the binary–ordered limit.

In Fig. (6) we have shown the same characteristics but for $x = 0.25$ near the segregation limit, i.e. $P_{AA} = 0.8125$, $P_{BB} = 0.9375$, $P_{AB} = 0.1875$ and $P_{BA} = 0.0625$. In general, we observe most peaked structures in LDOS in a case of random disorder and more smooth LDOS curves when some value of the short–range–order is introduced. Having calculated LDOS for different clusters we proceed to computing the mean–square charge fluctuations in the site occupation numbers. Results are shown in Figs. (7 – 11).

We display the charge fluctuations versus the Fermi energy level. In Figs. (7 – 8) we have displayed MSCF for $x = 0.25$ and increasing value of a disorder parameter on type–A atoms (upper panel), here minority sites, and on type–B atoms (lower panel), here majority sites. The site energies are $\varepsilon_A = -\varepsilon_B = 0.5$ eV and 2.0 eV for figures (7) and (8), respectively. We observe the largest fluctuations for a case with
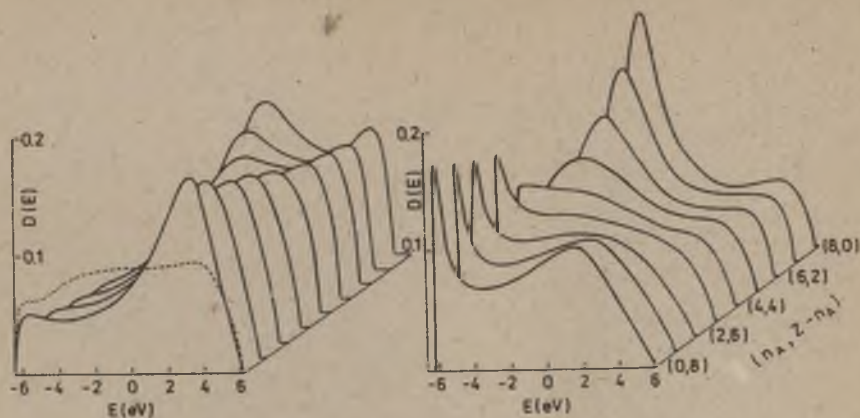
Fig. 3. The same as in Fig. (2) but for $p = 0$ (random disorder limit

largest disorder, i.e. for points which lie relatively close to the random disorder limit. We also observe, that for a greater scattering strength (SS) the MSCF are greater than for smaller values of SS. In addition, for small value of SS the MSCF has a form of the two peaked structure, without third maximum in upper part of the energy band. For greater SS the largest fluctuations appear in the middle and upper part of the band. In Fig. 9 we present MSCF for points on (x,p) plane (see Fig. (1)) lying along the line of a constant concentration of a type–A atoms, $x = 0.5$ and varying disorder parameter p (from nearly long–range–order limit to a random disorder case). For a point $x = 0.5$, $p = -1$ we have obtained MSCF a few order smaller than this one for greater values of the parameter p and we do not displayed it in this figure. The greatest MMSCF are observed for $p = 0$ and when we move towards smaller values of the parameter p $(p < 0)$ then the fluctuations are decreased. Only in a lower part of the energy band (for the fluctuations on a type–B atoms) one can observe another sequence of peaks (in comparison with MSCF on a type–A atom) but differences are rather small. In Figs. (10, 11) we present MSCF for $p = -\frac{1}{3}$ and $x = 0.5$, $x = 0.75$. The site energy ε_A is 1.0 eV in Fig. (10) and 2.0 eV in Fig. 11. First of all, we observe the general feature that with increasing value of the scattering strength the charge fluctuations increase. Additionally, for smaller values of SS and far away from the random disorder limit, the MSCF has a structure with two maxima (and not with three, as usual), without the maximum placed for Fermi energies lying in higher part of the energy band.

In conclusion, we have presented a theory of the static charge fluctuations in alloys with a short–range–order included. The charge fluctuations, as well as the local density of states was calculated within the method which treats part of the system exactly as a cluster of atoms and simulates the rest of a lattice by connecting to each cluster's surface atom a Bethe–lattice. Generally, the mean–square charge fluctuations calculated for a system with the short–range–order included are
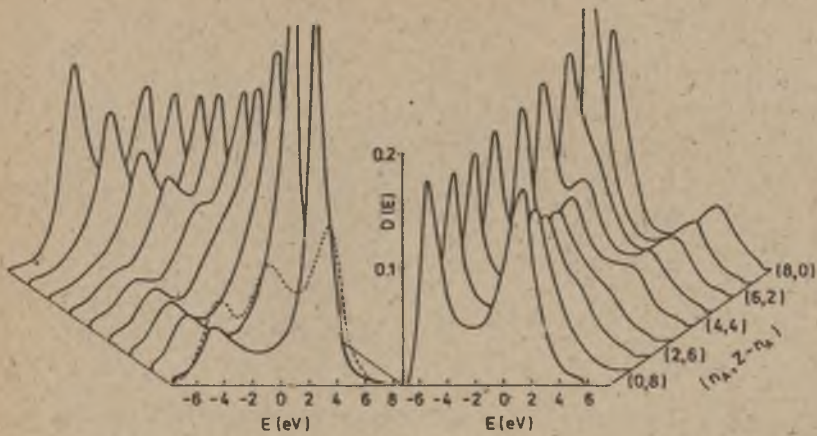
Fig. 4. The same as in Fig. (2) but for $x = 0.75$ and $p = 0$

reduced in comparison with fluctuations obtained for completely random disorder alloy. The results presented in this paper indicate, that the charge fluctuations for a long–range–order limit are a few orders smaller than for other values of the parameter describing the alloy's disorder. Also, for points (x, p) lying near the binary ordered limit the fluctuations are enhanced on majority sites, whereas on minority sites are depressed. Finally, the influence of the short–range–order on the charge fluctuations in alloys is significant, so any theoretical description of the experimental study of the real alloys systems for which the amount of a valence charge on an atom can be important, have to take this fact into account.
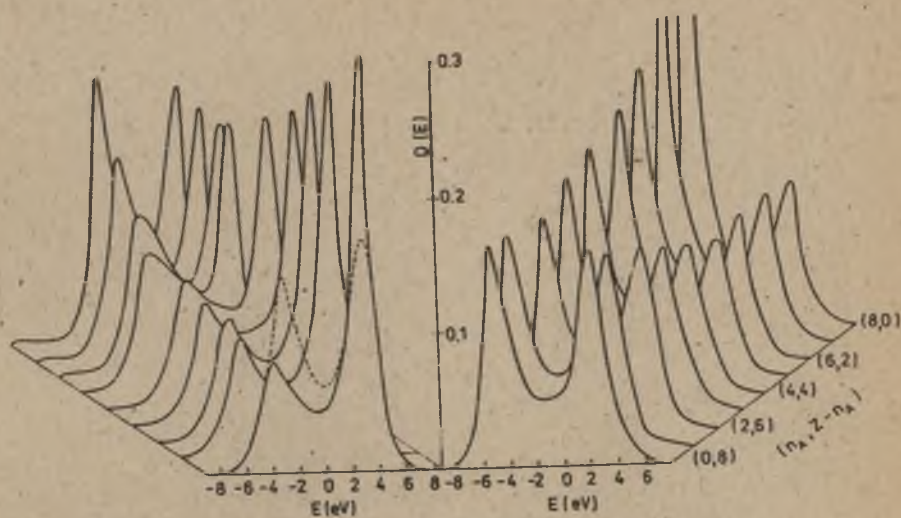
Fig. 5. The same as in Fig. (2) but for $x = 0.875$ and $p = 0$
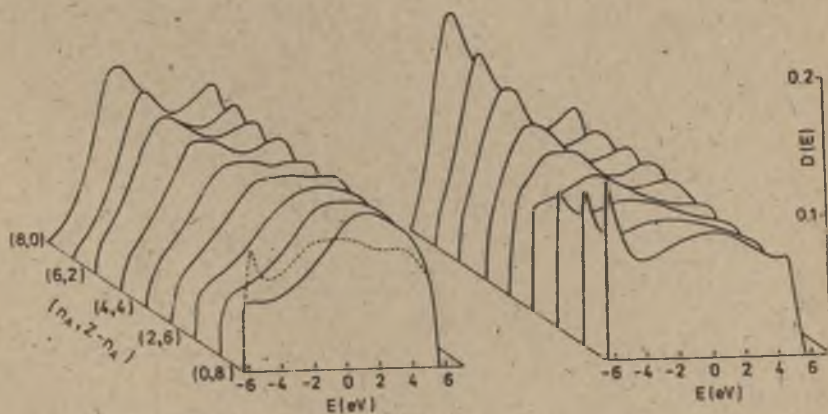
Fig. 6. The same as in Fig. (2) but for $x = 0.25$ and $p = 0.75$
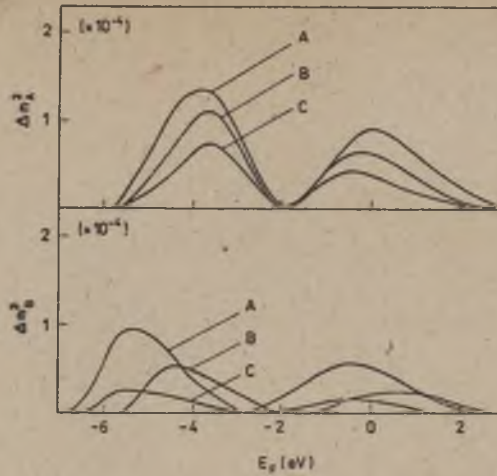
Fig. 7. Mean–square charge fluctuations on type–A atoms (upper panel) and on type–B atoms (lower panel) as a function of Fermi energy calculated for three different values of the short-range-order parameter $p = 0.5, 0.75$ and 0.875 (curves A, B and C, respectively) for $x = 0,25$ and $\varepsilon_A = -\varepsilon_B = 0.5$ eV
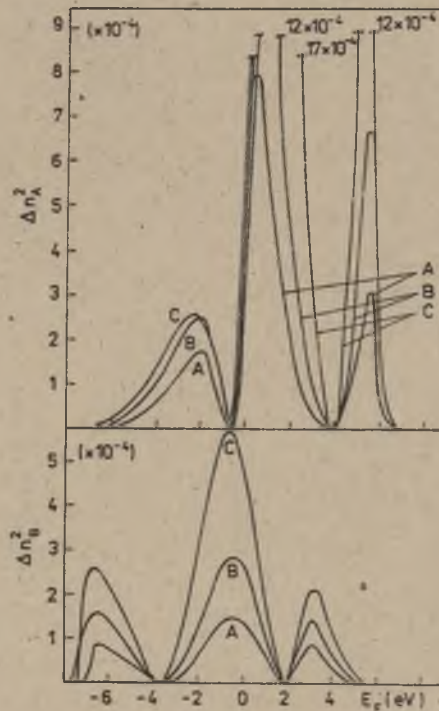
Fig. 8. The same as in Fig. (7) but for $\varepsilon_A = -\varepsilon_B = 2.0$ eV
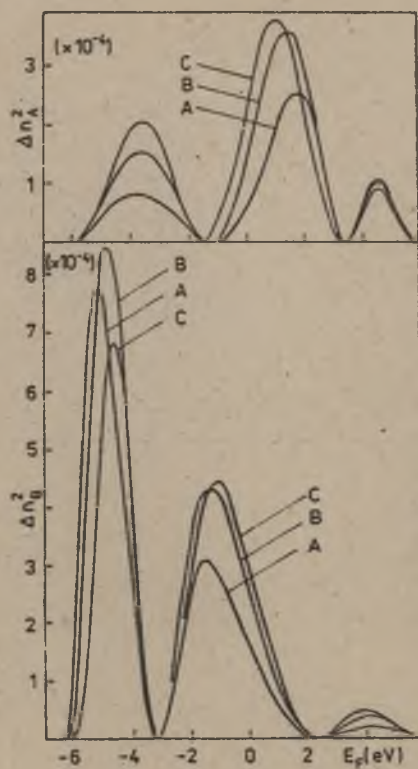
Fig. 9. The same as in Fig. (7) but for $x = 0.5$ and $p = -\dfrac{2}{3}, -\dfrac{1}{3}$ and 0.0 (curves A, B and C, respectively) for $\varepsilon_A = -\varepsilon_B = 1.0$ eV
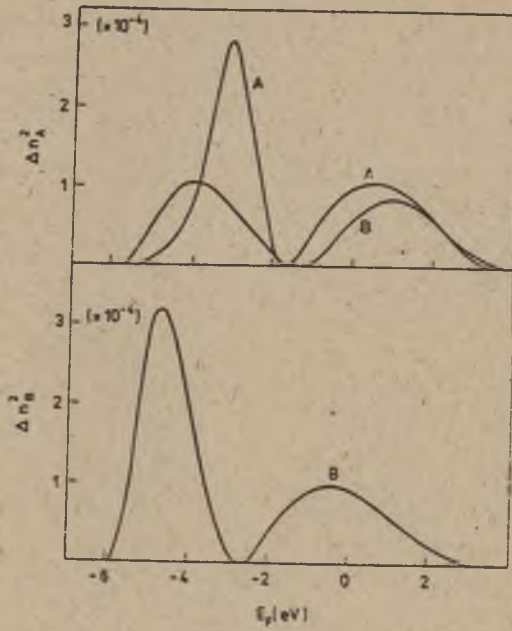
Fig.10. The same as in Fig. (7) but for $p = -\dfrac{1}{3}$, $x = 0.5$ and 0.75 (curves A, and B. respectively) for $\varepsilon_A = -\varepsilon_B \doteq 0.5$ eV. The charge fluctuations on minority atoms (i.e. on type-B atoms, lower panel) are a few orders smaller and not displayed here
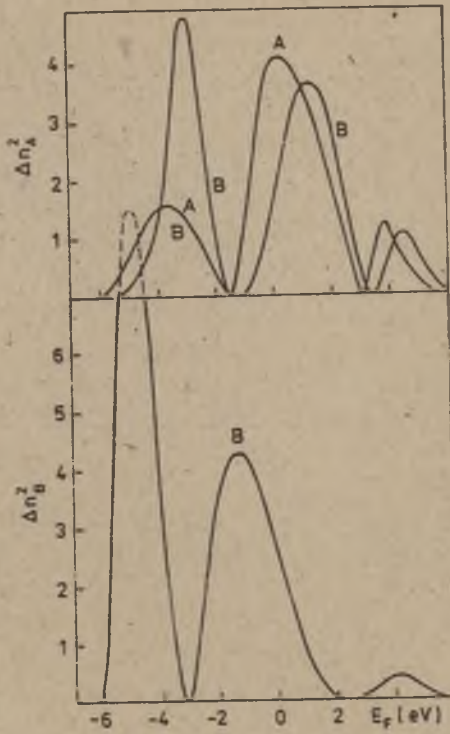
Fig. 11. The same as in Fig. (10) but for $\varepsilon_A = -\varepsilon_B = 1.0$ eV

REFERENCES

[1] Ling D.D., Gelatt C.D., *Phys. Rev.* B26, 2819 (1982)

[2] Hamada N., Miwa H., *Progr. Theoret. Phys.* Vol. 59, 1045 (1978)

[3] Parmigiani F., Samoggia G., *Europhys. Lett.* 7, 543 (1988)

[4] Velicky B., Kirkpatrick S., Ehrenreich H. *Phys. Rev.* 175, 747 (1968)

[5] Yonezawa F., Odagaki T., *J. Phys. Soc. Jpn* 47, 379 (1979); 47, 388 (1979)

[6] Montgomery C.G., *Phys. Rev.* B25, 7773 (1983)

[7] Tsukada M., *J. Phys. Soc. Jpn.* 26, 684 (1969); 32, 1475 (1972)

[8] Mills R., Ratanavararaksa R., *Phys. Rev.* B18, 5291 (1978)

[9] Katsura S., Takizawa M., *Progr. Theor. Phys.* 51, 82 (1974)

[10] Falicov L.M., Yndurain F., *Phys. Rev.* B12, 5664 (1975)

[11] Verges J.A., Yndurain F., *J. Phys. F.: Metal Phys.*, Vol. 8, 873 (1978)

[12] Robbins M.O., Falicov L.M., *Phys. Rev.* B25, 2343 (1982); B29, 1333 (1984)

[13] Chaudhuri P., Moitra R.K., *Phys. Rev.* B18, 6694 (1978)

[14] Chaudhuri P., Moitra R.K., *J. Phys.* C9, L455 (1976)

[15] Falicov L.M., Yndurain F., *Phys. Rev.* B12, 5664 (1975)

[16] Gómez – Santos G., *J. Phys.* C16, L453, (1983)

[17] Yndurain F., *Phys. Rev.* B18, 2876 (1978)

[18] Andriotis A.N., Lowther J.E., *J. Phys. F: Met. Phys.* 16, 1189 (1986)

[19] Sen P.N., Yndurain F., *Phys. Rev.* B13, 4387 (1976)

STRESZCZENIE

W pracy przedstawiono teorię fluktuacji ładunkowych w stopach dwuskładnikowych, charakteryzujących się istnieniem uporządkowania bliskiego zasięgu. Uporządkowanie to uwzględniono przy pomocy dokładnego rozważenia małej grupy atomów, natomiast wpływ pozostałej części kryształu opisany jest efektywną siecią krystaliczną typu drzewa Cayley'a. Przeprowadzono obliczenia numeryczne lokalnej gęstości stanów dla klasterów dziewięcioatomowych (o różnej konfiguracji atomów) oraz fluktuacji ładunku dla szerokiego zakresu parametrów charakteryzujących stopy. Fluktuacje ładunku są największe w przypadku stopów, które nie wykazują uporządkowania bliskiego zasięgu i znacznie maleją w miarę jego wzrostu. Duże fluktuacje ładunku zaobserwowano również w stopach wykazujących duże uporządkowanie typu A–B–A–B

W świetle uzyskanych wyników należy sądzic, że teoretyczny opis zjawisk fizycznych, w których wielkość ładunku zlokalizowanego na atomach stopu ma zasadnicze znaczenie, musi uwzględniać wpływ uporządkowania bliskiego zasięgu na wielkość tego ładunku.

РЕЗЮМЕ

В работе представлено теорию флуктуации заряда в бинарных сплавах характеризующихся существованием ближнего порядка. Упорядочение это учтено с

помощью точного описания малой группы атомов, а влияние остальной части кристалла описано эффективной кристаллической решёткой типа дерева Кейлея. Проведено машинные расчёты локальной плотности состояний для 9-ти атомных кластеров (о различной конфигурации атомов) и флуктуации заряда в случае широкого предела параметров описывающих сплавы. Флуктуации заряда самые большие для сплавов, в которых не существует ближний порядок и значительно уменьшаются по мере его возрастания. Большие флуктуации наблюдают рм цыдот ся тоже в сплавах, которые характеризуются большим упорядоченнем типа А–В–А–В.

Из наших результатов следует, что теоретическое описание физических явлений, в которых величина эффективного заряда локализованного на атомах сплава играет существенную роль, должно учитывать влияние ближнего порыадка на величину этого заряда.

Złożono 13. I. 1989.

ERRATA

W vol. LX/LXI „Annales UMCS, sectio AAA (Physica)" opuszczono nazwisko i ardres jednego ze współautorów pracy „Nonadiabatic and Dispative Effects in Low Energy Nuclear Fission" zamieszczonej na str. 361. Jest nim E. Werner z Institute of Theoretical Physics, University'of Regensburg.